THE COHERENT ROTATION OF π-ELECTRON IN A SMALL AROMATIC MOLECULE

Ho Quang Huy

Faculty of Engineering Technology, University of Phan Thiet, Lam Dong, Vietnam

Abstract: *Coherent rotation is a typical form of charge migration in aromatic molecules, in which π-electron rotates along the ring loop of molecule. Within a quantum-mechanical framework, the π-electron rotation can be characterized by the expectation values of observable operators, including angular momentum and current density. These quantities can be evaluated using analytical expressions combined with ab initio quantum-chemical calculations by Gaussian in H. Mineo, et al., (2013); an approach that is applicable to a wide range size of aromatic molecules. In this work, we apply this approach to investigate the coherent rotation of π-electron in a simple aromatic, s-triazine ($C_3H_3N_3$), which belongs to the D_{3h} symmetry group. Ring currents are identified not only along rings consisting of carbon-carbon atoms, or nitrogen-nitrogen atoms, but also along rings involving the nearest neighbor carbon-nitrogen pairs. The magnitude of bond current is determined from the total flux crossing a plane located at the midpoint of each bond connecting two atoms. To visualize the spatial distribution of the current density, current-density maps are plotted on a plane parallel to the molecular plane at a distance of z=1.0 Å.*

Keywords: *aromatic molecule coherent rotation, π-electron*

1. INTRODUCTION

Nowadays, the size of building blocks in electronic devices has been progressively reduced. In next-generation electronic devices, nanoscale materials (from approximately 1-100 nm) have been widely applied in device fabrication, such as transistors and solar cells (Kumar & Prakash, 2021; Mohammed et al., 2025). Furthermore, the miniaturization process has continued down to the molecular scale, reaching dimensions of several ångströms (Hsu et al., 2009, 2012). In the first decade of the 21st century, controlling electronic charge migration within individual molecules became a key issue in both theoretical and applied research (Krause et al., 2005; Barth et al., 2006; Kanno et al., 2006; Nobusada & Yabana, 2007; Ulusoy & Nest, 2011; Hermann et al., 2016; Jia et al., 2019). These studies have provided a flexible framework for controlling electronic currents, ranging from linear molecular systems (Krause et al., 2005; Jia et al., 2019) to aromatic ring molecular groups (Barth et al., 2006; Kanno et al., 2006; Nobusada & Yabana, 2007; Ulusoy & Nest, 2011; Hermann et al., 2016).

Coherent rotation is a typical form of charge migration involving π-electron (delocalized electron) in aromatic ring

molecules. Coherent rotation of π-electron originates from the excitation of a pair of electronic excited states induced by a UV laser pulse (Barth et al., 2006; Kanno et al., 2006). This rotation-induced ring current is an interesting candidate not only for studying aromaticity or antiaromaticity in a molecular systems (Steiner et al., 2001, 2005), but also for supporting the development of molecular devices, such as ultrafast switches (Mineo et al., 2012).

Coherent ring currents have been widely used to investigate a variety of aromatic molecular systems, ranging from single-ring to multi-ring structures, and from low-symmetry to high-symmetry groups, as demonstrated by Barth et al. (2006), Kanno et al. (2006). In these studies, the electronic structure of the molecular system is first determined by using *ab initio* quantum-chemical calculations. Subsequently, the time-dependent Schrödinger equation is solved numerically in the presence of an external laser field, yielding the time-dependent expectation values of observable operators associated with π-electron rotation, such as angular momentum and ring current.

On the other hand, Mineo and co-workers proposed an analytical approach to evaluate the expectation values of these quantities directly from molecular data obtained from *ab initio* calculations using the Gaussian program (Mineo et al., 2013). In particular, the magnitude of the coherent current can be evaluated along the chemical bonds in a molecular ring. This approach provides a clearer physical picture, since the current density is distributed in the vicinity of chemical bonds, and the set of bonds arranged around the molecular ring naturally forms a ring-current pattern.

However, the above approach has so far been applied mainly to homogeneous atomic systems, such as P-2,2'-biphenol (Mineo et al., 2013), in which the bond current is evaluated between carbon-carbon atoms. In the present study, we extend this approach to an inhomogeneous atomic system, s-triazine ($C_3H_3N_3$), in which the bond current is evaluated not only between atoms of the same type but also between atoms of different types.

The paper is organized as follows. Section 2 presents the derivation of the expressions for the bond current and the current-density vector, following the approach described in Mineo et al. (2013). Section 3 presents and discusses the bond currents and the corresponding current-density maps for s-triazine. Finally, Section 4 summarizes the main results and outlines possible future developments of this approach.

2. LITERATURE REVIEW AND RESEARCH METHODS

In this section, we briefly describe the measurement of the coherent rotation by presenting the analytical expressions of the current density vector and for the magnitude of the bond current crossing a plane at the midpoint between two atoms. The derived formulas can be applied to a wide class of the aromatic molecules, including benzene

(radius of ring is 1.39 Å), (P)-2,2'-biphenol (two connected rings) (Mineo et al., 2013), anthracene (the length of anthracene is 8.40 Å) (Mineo & Fujimura, 2017).

A molecule consists of electrons and nuclei, with the number electron is and number atom is N_A. The electrons exhibit highly mobile motion in the extremely slow variation of the nuclei. Within the adiabatic approximation, the electron dynamics can be investigated while the nuclear geometrical configuration is frozen. As a result, the electronic states are described by the time-independent Schrödinger equation as follows:

$$\widehat{H}_0\Phi_\alpha = \varepsilon_\alpha\Phi_\alpha, \qquad (1.1)$$

here, the Hamiltonian of a free molecule can be expressed as $\widehat{H}_0 = \widehat{K} + V_{e-e} + V_{N-e}$. The first term is the total kinetic operator of all electron, which is written as follows

$$\widehat{K} = \sum_{j=1}^{N} \frac{\widehat{\boldsymbol{p}}_j{}^2}{2m_e}, \qquad (1.2)$$

the second term is the Coulomb repulsion interaction electrons

$$V_{e-e} = \frac{e^2}{4\pi\varepsilon_0}\sum_{j=1}^{N}\sum_{k<j}^{N}\frac{1}{|\boldsymbol{r}_j - \boldsymbol{r}_k|}, \qquad (1.3)$$

with $\boldsymbol{r}_j$ and $\boldsymbol{r}_k$ are the position vector of *j*-th electron and *k*-th electron, respectively.

The third term describes the Coulomb attraction interaction between nuclei and electrons is

$$V_{N-e} = \frac{e^2}{4\pi\varepsilon_0}\sum_{J=1}^{N_A}\sum_{j=1}^{N}\frac{-Z_J}{|\boldsymbol{R}_J - \boldsymbol{r}_j|}, \qquad (1.4)$$

with $\boldsymbol{R}_J, r_j$ are the position vector of *J*-th nuclei and *j*-th electron. In Eqs. (1.2)-(1.4), m_e and *e* denote the mass and charge of electrons, respectively.

Eq. (1.1) yields a set of eigenstates, Φ_α and eigenvalues, ε_α (with $\alpha = 0, 1, 2, ...$), which correspond to the wave functions and energies of the α-th electronic state. The ground electronic state is written as a Slater-determinant of the occupied molecular orbitals (MOs) in a closed-shell system (with an even number of electrons),

$$\Phi_0 = \|\phi_1(\boldsymbol{r}_1)\sigma_\uparrow \quad \phi_1(\boldsymbol{r}_2)\sigma_\downarrow \quad ... \quad \phi_a(\boldsymbol{r}_k)\sigma_p \quad ... \quad ... \quad \phi_{N/2}(\boldsymbol{r}_{N-1})\sigma_\uparrow \quad \phi_{N/2}(\boldsymbol{r}_N)\sigma_\downarrow\|, \qquad (2)$$

Here, $\boldsymbol{r}_k$ denotes the position vector of the *k*-th electron in system; $\phi_a(\boldsymbol{r}_k)$ represents the spatial wave function of the a-th occupied MO, and σ_p is the spin-wave function with $p = \uparrow (\downarrow)$ denoting spin-up (spin-down) state.

The higher-energy electronic states (excited states) are expressed as

$$\Phi_\alpha = \sum_{a,a'} c_{aa'}^{(CI)} \Phi_{a\to a'}^{(1)} + \sum_{p<q} \sum_{p'<q'} c_{pp';qq'}^{(CI)} \Phi_{p\to p';q\to q'}^{(2)} + \cdots , \quad (3)$$

where the first summation includes singly excited determinant. In a singly excited determinant $\Phi_{a\to a'}^{(1)}$ an occupied a-MO is promoted by an unoccupied a'-MO; $c_{aa'}^{(CI)}$ denotes the corresponding configuration-interaction (CI) coefficient. The second summation includes a doubly excited determinant. In this study, only the contributions from singly excited state determinants are considered, since their configuration weights are typically significantly larger.

In Eq.(2), a MO, $\phi_k(\boldsymbol{r})$ is expanded as a linear combination of atomic orbitals (LCAO), $\chi_I(\boldsymbol{r}-\boldsymbol{R}_I)$ centered on the atoms of the molecule,

$$\phi_k(\boldsymbol{r}) = \sum_{I=1}^{N_A} c_{k,I}\chi_I(\boldsymbol{r}-\boldsymbol{R}_I) , \quad (4)$$

where $c_{k,I}$ denotes the molecular orbital coefficient of the atomic orbital on the I-th atom. In the Hückel model, π-type MOs are described as linear combinations of p_z-type AOs, with the z-axis perpendicular to the molecular plane (Atkins & Friedman, 2005).

When a molecule is free in space, the electrons occupy only the ground electronic state. However, when the molecule is applied by an external field, such as a UV laser pulse, the interaction between the molecular electrons and the laser electronic field is described by a time-dependent potential $V(t)$. As a result, excited states become populated, and the wave function can be expanded as a linear combination of electronic states

$$\Phi(t) = c_0(t)\Phi_0 + \sum_\alpha c_\alpha(t)\Phi_\alpha . \quad (5)$$

The time-dependent coefficient $c_\alpha(t)$ gives the population of the α-th excited electronic state through $|c_\alpha(t)|^2$.

In coherent excitation process, a UV laser pulse synchronously excites a pair of optically allowed excited electronic states via a classical light-matter interaction within the dipole approximation, as illustrated in Fig. 1. For high-symmetry aromatic molecules, a pair of degenerate electronic states is selectively excited using a circularly polarized UV pulse (CP UV pulse) whose carrier frequency matches the energy gap between the ground state and these excited states. Their superpositions, either in-phase or out-phase, are also eigenstates of the angular momentum operator. Consequently, a unidirectional rotation of the π-electrons is triggered by left-handed or right-handed CP pulses.

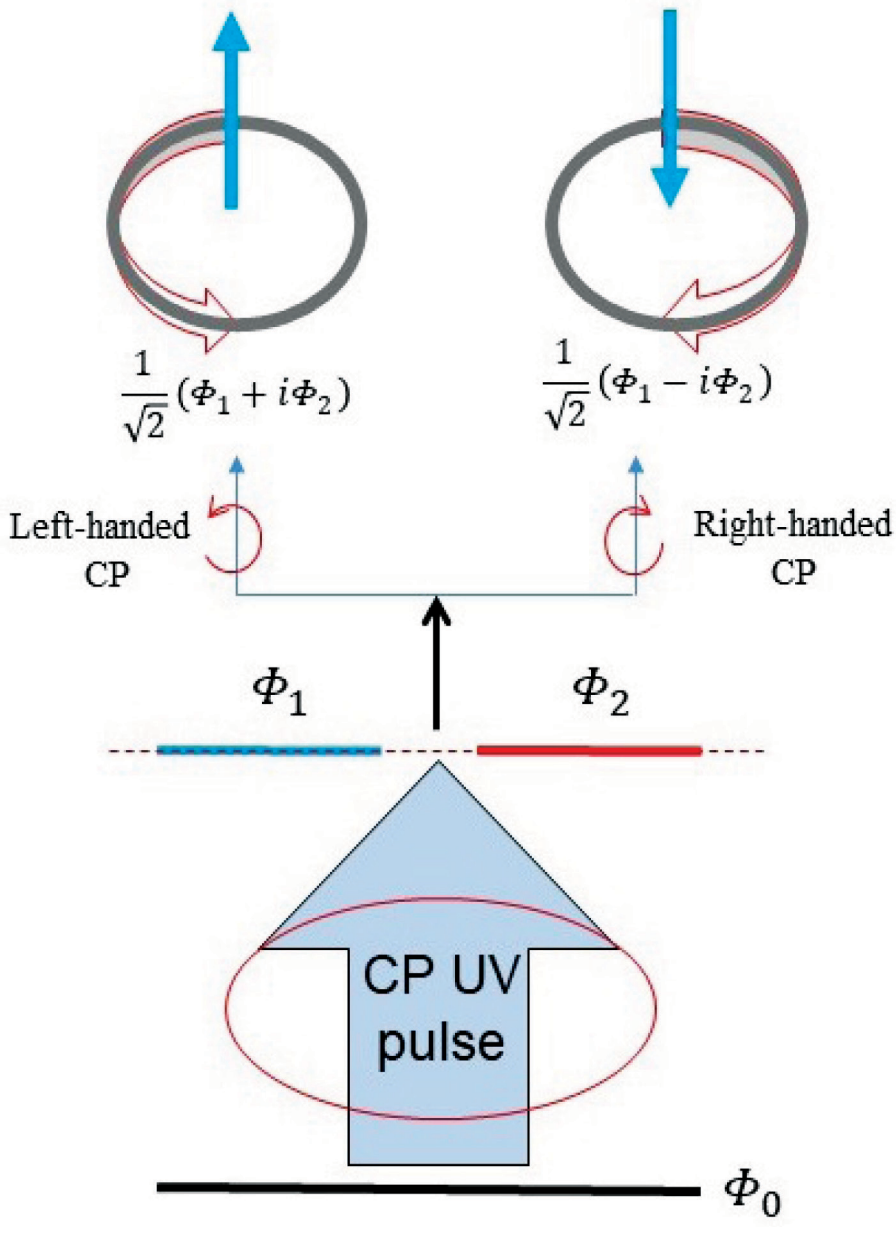

Figure 1. Coherent excitation of a pair of degenerate excited states by a circularly polarized UV pulse (CP UV pulse). A right-handed (left-handed) CP pulse selectively accesses the out-phase (in-phase) superposition of Φ_1 and Φ_2, corresponding to eigenstates of angular momentum operator with clockwise (counterclockwise) π-electron rotation

The expectation value of the current-density operator is defined as

$$\langle \boldsymbol{j}(\boldsymbol{r},t)\rangle = \langle \Phi(t)|\hat{\boldsymbol{j}}|\Phi(t)\rangle, \qquad (6.1)$$

the single-particle current-density operator is given by

$$\hat{\boldsymbol{j}} = \sum_{k=1}^{N}(-e)\frac{\hbar}{2m_e i}\left(\delta(\boldsymbol{r}-\boldsymbol{r}_k)\vec{\nabla}_k - \overleftarrow{\nabla}_k\delta(\boldsymbol{r}-\boldsymbol{r}_k)\right), \qquad (6.3)$$

with the Dirac-delta function $\delta(\boldsymbol{r}-\boldsymbol{r}_k)$ accounts for the contribution of the -th electron to the current-density vector at the observation position $\boldsymbol{r}$. The nabla operator $\overrightarrow{\nabla}_k$ ($\overleftarrow{\nabla}_k$) acts on the coordinates $\boldsymbol{r}_k$ of the k-th electron in the right-hand (left-hand) functions.

Therefore, the expectation value of the current-density vector can be written more explicitly as

$$\langle \boldsymbol{j}(\boldsymbol{r},t)\rangle = (-e)\frac{\hbar}{2m_e i}\int d^{3N}r \sum_{k=1}^{N}\delta(\boldsymbol{r}-\boldsymbol{r}_k)[\Phi^*(t)\nabla_k\Phi(t)-\Phi(t)\nabla_k\Phi^*(t)], \qquad (6.2)$$

where the multiple integral is evaluated over the -dimensional configuration space of all electrons in the molecule, denoted by $r=(\boldsymbol{r_1};\boldsymbol{r}_2;\ldots;\boldsymbol{r}_N)$.

When a circularly polarized ultraviolet (CP-UV) pulse excites a pair of degenerate electronic states, Φ_1 and Φ_2 ($\varepsilon_1=\varepsilon_2$), coherent rotation of the π electron is generated, as shown in Fig. 1. The expectation value of current-density operator is then given by

$$\langle \boldsymbol{j}(\boldsymbol{r},t)\rangle = (-e)\frac{\hbar}{m_e}\mathrm{Im}[c_2^*(t)c_1(t)]\int d^{3N}r \sum_{k=1}^{N}\delta(\boldsymbol{r}-\boldsymbol{r}_k)(\Phi_2\nabla_k\Phi_1-\Phi_1\nabla_k\Phi_2), \qquad (7)$$

by substituting Eq.(3) into Eq.(7), we obtain

$$\langle \boldsymbol{j}(\boldsymbol{r},t)\rangle = 2(-e)\frac{\hbar}{m_e}\mathrm{Im}[c_2^*(t)c_1(t)]\times \times\sum_{\{a,a',b,b'\}} c_{aa'}^{(\mathrm{CI})}c_{bb'}^{(\mathrm{CI})}\left[\delta_{ab}\left(\phi_{a'}(\boldsymbol{r})\nabla\phi_{b'}(\boldsymbol{r})-\phi_{b'}(\boldsymbol{r})\nabla\phi_{a'}(\boldsymbol{r})\right)+ +\delta_{a'b'}\left(\phi_a(\boldsymbol{r})\nabla\phi_b(\boldsymbol{r})-\phi_b(\boldsymbol{r})\nabla\phi_a(\boldsymbol{r})\right)\right]. \qquad (8)$$

The appearance of the factor of 2 in Eq.(8) originates from spin degeneracy in the Slater determinant of Eq.(2). The LCAO is adopted to represent the MOs in Eq.(8), namely and $\phi_a,\phi_b,\phi_{a'}$ and ϕ_b', yielding

$$\langle \boldsymbol{j}(\boldsymbol{r},t)\rangle = 2(-e)\frac{\hbar}{m_e}\mathrm{Im}[c_2^*(t)c_1(t)]\times \times\sum_{K=1}^{N_A}\sum_{I=1}^{N_A}\left[\sum_{\{a,a',b,b'\}} c_{aa'}^{(CI)}c_{bb'}^{(CI)}(\delta_{ab}c_{a'K}c_{b'I}+\delta_{a'b'}c_{aK}c_{bI})\right]\times \times[\chi_K(\boldsymbol{r}-\boldsymbol{R}_K)\nabla\chi_I(\boldsymbol{r}-\boldsymbol{R}_I)-\chi_I(\boldsymbol{r}-\boldsymbol{R}_I)\nabla\chi_K(\boldsymbol{r}-\boldsymbol{R}_K)], \qquad (9)$$

where K and I label atoms among the N_A atoms of the molecule, the set $\{a,a',b,b'\}$ runs over the set of MOs involved in the relevant excited states.

The flux of the current-density vector crossing a plane S is defined by

$$\langle J(t)\rangle = \iint d^2r_\perp \boldsymbol{n}.\langle \boldsymbol{j}(\boldsymbol{r},t)\rangle ; \qquad (10)$$

when the plane S is perpendicular to the line connecting atoms I- and K-th atom, the unit normal vector $\boldsymbol{n} \equiv (\boldsymbol{R}_I - \boldsymbol{R}_K)/|\boldsymbol{R}_I - \boldsymbol{R}_K|$ is perpendicular to the plane S.

In this case, the bond-current, introduced by Mineo et al., (2013), can be obtained by separating the contributions of the terms involving the I, K-th atoms pair in summation of Eq.(8), yielding

$$\langle \mathrm{J}(t)\rangle_{IK} = 2(-e)\frac{\hbar}{m_e}\mathrm{Im}[c_2^*(t)c_1(t)] \sum_{a,a',b,b'} c_{aa'}^{(CI)} c_{bb'}^{(CI)} \times$$
$$\times \left(\delta_{ab}\left(c_{a',K}c_{b',I} - c_{a',I}c_{b',iK}\right) + \delta_{a'b'}\left(c_{a,K}c_{b,I} - c_{a,I}c_{b,K}\right)\right)$$
$$\times \iint d^2r_\perp \boldsymbol{n}.[\chi_K(\boldsymbol{r}-\boldsymbol{R}_K)\nabla\chi_I(\boldsymbol{r}-\boldsymbol{R}_I) - \chi_I(\boldsymbol{r}-\boldsymbol{R}_I)\nabla\chi_K(\boldsymbol{r}-\boldsymbol{R}_K)]. \qquad (11)$$

3. RESULTS AND DISCUSSION

We adopt the coherent rotation treatment to evaluate the magnitude of bond currents in s-triazine ($C_3H_3N_3$). This molecule possesses D_{3h} symmetry (high symmetry), and is a planar aromatic molecule, in which three carbon atoms and three nitrogen atoms are arranged at the vertices of an irregular hexagon. The geometrical structure of the molecule is optimized using density functional theory (DFT) with the B3LYP functional and basis set cc-pVDZ using Gaussian09 (Gaussian, Inc., n.d.). The hexagonal ring is placed in the xy plane of the Cartesian coordinate system (z=0), as shown in Fig. 2(a). The bond currents between carbon-carbon, nitrogen-nitrogen, and carbon-nitrogen bond pairs are evaluated using Eq. (8). The distribution of current-density vectors has been plotted in a plane parallel to the xy plane at z=1.0 Å.

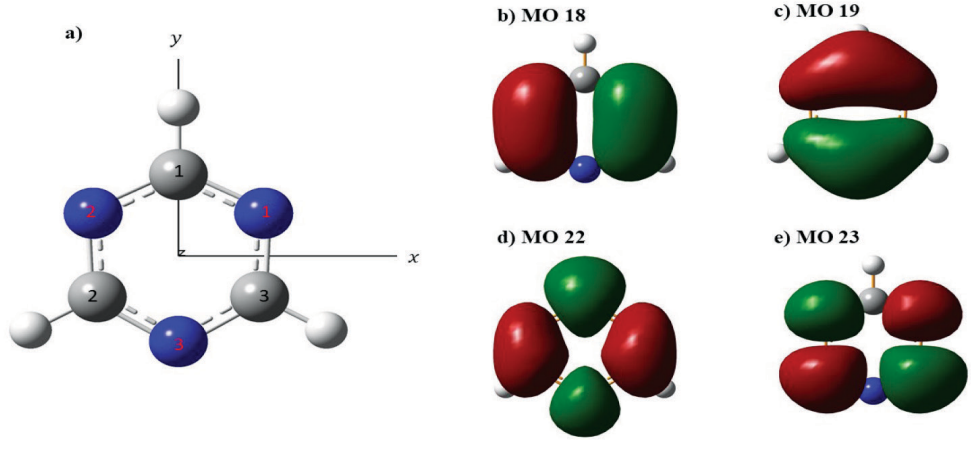

Figure 2. a) The optimized geometrical configuration of s-triazine belonging to the D_{3h} symmetry group. b)-e) Shapes of MO 18, 19, 22 and 23

The TD-DFT calculations were performed using the B3LYP functional and cc-pVDZ basis set at the fixed optimized geometry of the molecule. The results provide the excitation energies, transition dipole moments, the dominant molecular-orbital (MO) transitions: $k \rightarrow k'$, and the corresponding CI coefficients. The selected pairs of degenerate excited states are listed in Table 1. In particular, the transition dipole moment vectors of states S_9 and S_{10} are oriented along the *x*- and *y*-axes, respectively. The wave functions of these electronic excited states are each composed of two dominant MO transitions with equal weights, given by $2\left|c_{kk'}^{(CI)}\right|^2 = 48\%$. For S_9, the dominant MO transitions arise from the transitions: 18 (e") → 22 (e") and MO 19 (e") → 23 (e"). In contrast, for S_{10}, the dominant contributions correspond to the transitions: MO 18 (e") → 23 (e") and MO 19 (e") → 22 (e"). The shapes of the relevant MOs (18, 19, 22 and 23) are shown in Fig. 2 (b)-2(e).

Table 1. The molecular data from TDDFT/B3LYP PVDZ

Excited state	IRRep.†	Energy (in eV)	Transition dipole moment vector (in a.u.)			Dominant MO transition	$c_{kk'}^{(CI)}$
			μ_x	μ_y	μ_z	*k*-th MO → *k'*-th MO	
S_9	E'	7.76	-1.40	0.00	0.00	18 → 22	-0.489
						19 → 23	0.489
S_{10}			0.00	1.40	0.00	18 → 23	0.489
						19 → 22	0.489

Source: calculated by TDDFT/B3LYP in Gaussian (Gaussian, Inc., n.d.)
† Irreducible representation of excited states

In Table 2, the magnitude of the bond current is evaluated at the time when the quantity $\mathrm{Im}[c_2^*(t)c_1(t)]$ reaches its maximum value (=1/2) during the interaction with the CP pulse. The quantities $\langle \mathrm{J}(t)\rangle_{IK}^{(C)}$, $\langle \mathrm{J}(t)\rangle_{IK}^{(N)}$ and $\langle \mathrm{J}(t)\rangle_{Ik}^{(NC)}$ denote the bond current between carbon-carbon, nitrogen-nitrogen, nearest neighbor carbon-nitrogen pairs within the hexagonal ring, respectively.

For nearest-neighbor carbon-nitrogen pairs along the bonds of the molecular ring, the magnitudes of the bond current for pairs located symmetrically with respect to the *y*-axis are identical, (C_2-N_3 and N_3-C_3, N_2-C_2 and C_3-N_1, C_1-N_2 and N_1-C_2), because the *y*-axis is a principal symmetry axis of the D_{3h} point group. A similar symmetry relation is observed for carbon-carbon pairs (C_1-C_2 and C_3-C_1) and nitrogen-nitrogen pairs (N_2-N_3 and N_3-N_1).

The magnitudes of the bond currents flowing along the nearest-neighbor carbon-nitrogen pairs, carbon-carbon, and

nitrogen-nitrogen pairs are 291.6, 227.1 and 126.7 μA, respectively. The bond current in the carbon-carbon pair is slightly smaller than that in the nearest-neighbor carbon-nitrogen pair. In contrast, the nitrogen-nitrogen bond current is approximately half of the carbon-carbon bond current. These results indicate that the magnitude of bond currents is enhanced in the presence of two different types of atoms.

For the nearest-neighbor carbon-nitrogen bonds, the bond currents of C_1-N_2, N_2-C_2 and C_2-N_3 differ by approximately 0.005 μA (5 nA), even though these bonds are formally equivalent. A similar trend is observed for the carbon-carbon bond pairs and nitrogen-nitrogen bond pairs are about 3 nA in each case. These small variations can be attributed to differences in the overlap between pairs of MOs contributing to the bond currents, as seen in Eq. (11).

For S_9 and S_{10}, MOs 22 and 23 overlap in the transitions originating from the same occupied MOs, while MOs 18 and 19 overlap in the transitions terminating at the same unoccupied MOs. Because the molecular point group of s-triazine is D_{3h}, the bonds are not equivalent in the same sense as in benzene (D_{6h}). As a result, the overlaps between pairs of MOs differ slightly among these positions, leading to small differences in the corresponding bond currents.

For comparison, in a homogeneous atomic system, 2,2'-P-biphenol, Mineo et al. (2013) reported a maximum carbon-carbon bond current of about 181 μA using *ab initio* calculation with the 6-31G+(d, p) basis set. Therefore, the magnitudes of bond currents in 2,2'-P-biphenol and s-triazine are of the same order (several hundred microamperes). In 2,2'-P-biphenol, the current primarily flows along the nearest-neighbor carbon-carbon bond pairs within the molecular rings. In contrast, in s-triazine, the current flows not only along the molecular ring, but also along carbon-carbon and nitrogen-nitrogen pairs located outside the molecular ring. Consequently, the molecular ring is no longer the sole current pathway in inhomogeneous molecular systems.

Table 2. The magnitude of bond current is evaluated at the time of maximum coherence, $\mathbf{Im}[c_2^*(t)c_1(t)] = 1/2$

a) Nearest neighbor carbon-nitrogen pair

I-th atom – K-th atom	C_1-N_2	N_2-C_2	C_2-N_3	N_3-C_3	C_3-N_1	N_1-C_1
$\langle J(t)\rangle_{lk}^{(C)}$ (μA)	291.635	291.640	291.630	291.630	291.640	291.635

b) Carbon-carbon (C_I-C_K) and Nitrogen-nitrogen (N_I-N_K)

C_I- C_K	C_1-C_2	C_2-C_3	C_3-C_1
$\langle J(t)\rangle_{Ik}^{(C)}$ (μA)	227.106	227.109	227.106
N_I-N_K	N_1-N_2	N_2-N_3	N_3-N_1
$\langle J(t)\rangle_{Ik}^{(C)}$ (μA)	126.659	126.656	126.656

*Source: calculated by Eq.(11) and molecular data from Gaussian (*Gaussian, Inc., n.d.*)*

The current-density maps are plotted using the *quiver* function in the Matplotlib library, with the same scale factor for the length of vectors. The regions of these plots are set up over -2.0 Å < x < 2.0 Å and -2.0 Å < y < 2.0 Å. A uniform grid of 40 points is used along each axis. The current-density vector is calculated using Eq. (9). In Fig. 3, subfigures (a), (b), and (c) represent the contributions from carbon atoms only, nitrogen atoms only, and nearest-neighbor carbon-nitrogen pairs along the ring, respectively. Fig. 3(d) includes contributions from all of the atoms in the molecule.

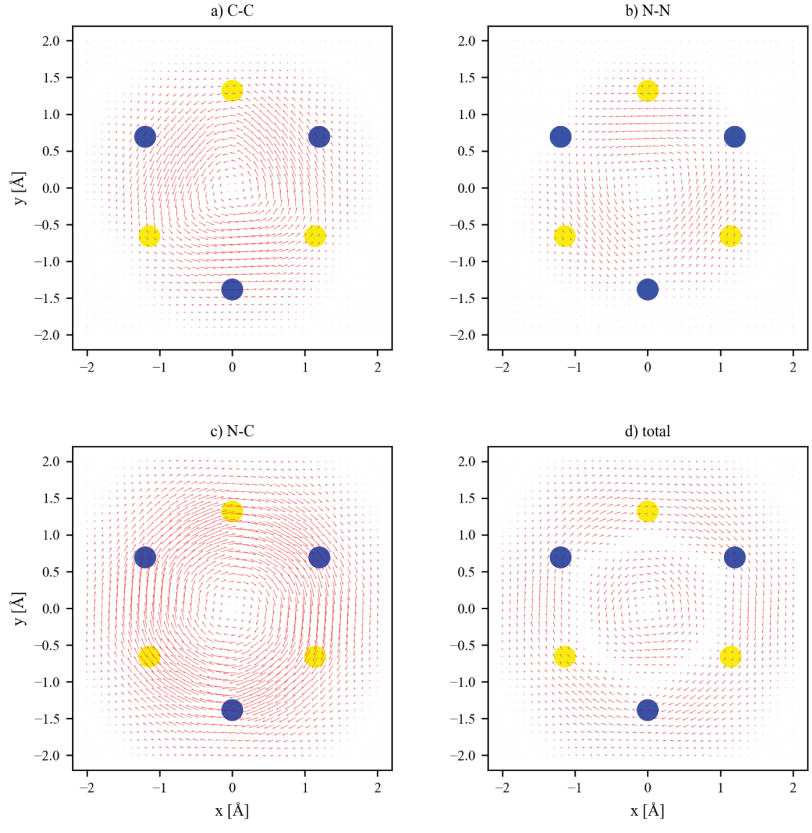

Figure 3. Current-density maps plotted for (a) contributions from carbon atoms only, (b) contributions from nitrogen atoms only, (c) the nearest-neighbor carbon-nitrogen pairs in the molecular ring, (d) contributions from all atoms in s-triazine. Yellow and blue circles denote the positions of carbon and nitrogen atoms, respectively

The directions of current-density vectors in Fig. 3(c) are opposite to those in Fig. 3(a) and 3(b). In Fig. 3(c), the current-density vectors flow clockwise, whereas they flow counterclockwise in Fig. 3(a) and 3(b). Moreover, the current-density vectors in Fig. 3(a) are longer than those in Fig. 3(b), consistent with the larger magnitude of the bond current $\langle \mathrm{J}(t) \rangle_{Ik}^{(C)}$ compared to $\langle \mathrm{J}(t) \rangle_{IK}^{(N)}$.

In all three subfigures of Figs. 3(a)-3(c), the magnitudes of the current-density vectors initially increase with radial distance, reach a local maximum, and then decrease as the distance extends from the inner to the outer region of the molecular ring. In each case, the region around this local maximum exhibits an approximately annular distribution, which we here define as the concentrated ring-current region. The local maximum magnitudes of the current density in Fig. 3(a), (3b) and (3c) are 0.77, 0.50, and 1.51 (a.u.), respectively, occurring at radial distances of 2.11, 2.11, 2.32 (Å) from the origin (x=0, y=0). In Fig. 3(d), which shows the total current density vectors, the maximum magnitude is 0.43 (a.u.) at a radial distance of 2.50 Å. For comparison, P. W. Flower and E. Steiner (1997) reported that a maximum magnitude of current density is 0.078 (a.u.) for π-electron current in s-triazine. In the present study, the maximum total coherent current density is therefore more than six times larger. This difference can be understood from the distinct physical origins of the two types of current. In the traditional study by Steiner and Flower, the ring current arises as a response to an external static magnetic field, where the interaction between the ring current-induced magnetic dipole moment and the magnetic field is treated as a perturbation term (Steiner et al., 2001). In contrast, the coherent current considered here is generated by directly exciting the pair of degenerate excited states in a laser field (Fig. 1), in which the interaction between the laser field and the electronic dipole moment of the molecular system is explicitly included (Barth et al., 2006).

Here, the concentrated ring-current region of the N-C bond (Fig. 3(c)) is located farther outward than those associated with the C-C (Fig. 3(a)) and the N-N (Fig. 3(b)). As a result, in Fig. 3(c), the current-density vectors are longer in the outer region of the molecular ring, but become shorter than toward the inner region. By contrast, in Figs. 3(a) and 3(b), the longest current-density vectors are found in the inner region of the ring. Consequently, in Fig. 3(d), two oppositely directed current patterns appear in the inner ring flow counterclockwise, whereas those in the outer ring flow clockwise.

In this study, the degenerate pair of excited states S_9 and S_{10} is coherently excited by a CP pulse to form the superposition state $(S_9 - iS_{10})$. However, the transition dipole moment of S_9 is oriented along the negative x-axis, whereas that of S_{10} is oriented along the positive y-axis. As a result, the wave functions of S_9 and S_{10} correspond to $(-1)\Phi_1$ and Φ_2 , respectively. Consequently, the resulting

superposition state is $(\Phi_1 + i\Phi_2)/\sqrt{2}$, with the coherence term $\mathrm{Im}[c_2^*(t^*)c_1(t^*)] = 1/2$ at the end of the pulse. As illustrated in Fig. 1, this superposition state describes a counterclockwise rotation of π-electron. Owing to the negative charge of the electron, the corresponding ring current flows clockwise, which is shown as the direction of vectors in the current-density map.

Finally, it is important to note that the bond currents may arise independently of the conventional chemical bond paths of the molecule. In particular, nonzero bond currents are also obtained for C-C and N-N pairs, even though these pairs do not correspond to formal bonded interactions in the usual chemical bonding.

4. CONCLUSION AND IMPLICATIONS

In this study, bond currents and current-density vectors in s-triazine have been investigated under coherent excitation of the pair of degenerate excited states. The magnitude of the bond current is found to be notable not only along the carbon-nitrogen bonds on the molecular ring but also for the non-bonded pairs, such as carbon-carbon and nitrogen-nitrogen pairs. In particular, the carbon-carbon bond current is approximately twice as strong as the nitrogen-nitrogen bond current. The current-density vectors are distributed over two concentric separate rings, namely an inner ring and an outer ring, with opposite flow directions. The current density flowing along the nearest-neighbor carbon-nitrogen bonds on the molecular ring provides the dominant contribution to the outer ring, while the current density between carbon-carbon and nitrogen-nitrogen pairs contributes mainly to the inner ring.

These results are obtained using the present analytical approach for s-triazine, which is a typical example of an inhomogeneous atomic system composed of two different atomic species, carbon and nitrogen. However, the origin of the separation into two ring currents in s-triazine has not yet been fully understood within this framework. As a direction for future work, this approach will be extended for the investigation of the impact of different atomic species in other inhomogeneous aromatic systems on the formation of coherent ring currents.

Acknowledgments: *We are grateful to Dr. Hirobumi Mineo (Van Lang University) for his useful comments on the analytical expressions of the bond currents and current-density vectors.*

Author Information:

M.A. Quang Huy Ho *(*Corresponding author)*, Faculty of Engineering and Technology, University of Phan Thiet, Lam Dong Province, Vietnam.

Email: hqhuy@upt.edu.vn

Article Information:
Received: February 15, 2026
Revised: May 14,2026
Accepted: May 15, 2026

Note
The author declares no competing interests regarding this article

REFERENCES

Atkins, P., & Friedman, R. (2005). Molecular orbital theory of polyatomic molecules. In *Molecular quantum mechanics* (4th ed., p. 266). Oxford University Press.

Barth, I., Manz, J., Shigeta, Y., & Yagi, K. (2006). Unidirectional electronic ring current driven by a few-cycle circularly polarized laser pulse: Quantum model simulations for Mg-porphyrin. *Journal of the American Chemical Society, 128*, 7043–7049. https://doi.org/10.1021/ja0571971

Frisch, M. J., Trucks, G. W., Schlegel, H. B., & co-authors. (2016). *Gaussian 09* [Computer software]. Gaussian, Inc. https://www.gaussian.com/g09citation/

Flowler, P. W., and Steiner, E. (1997). Ring Currents and Aromaticity of Monocyclic π-Electron Systems C_6H_6, $B_3N_3H_6$, $B_3O_3H_3$, $C_3N_3H_3$, $C_5H_5^-$,$C_7H_7^+$,$C_3N_3F_3$,$C_6H_3F_3$, and C_6F_6. *The Journal of Physical Chemistry A*, *101*, 1409-1413. https://pubs.acs.org/doi/10.1021/jp9637946

Hermann, G., Liu, C., Manz, J., & co-authors. (2016). Multidirectional angular electronic flux during adiabatic attosecond charge migration in excited benzene. *The Journal of Physical Chemistry A, 120*, 5360–5369. https://doi.org/10.1021/acs.jpca.6b01948

Hsu, L.-Y., Huang, Q.-R., & Jin, B.-Y. (2009). Charge transport through a single molecular wire based on linear multimetal complexes: A non-equilibrium Green's function approach. *The Journal of Physical Chemistry C, 112*, 10538–10541. https://doi.org/10.1021/jp801926d

Hsu, L.-Y., & Rabitz, H. (2012). Single-molecule phenyl-acetylene-macrocycle-based optoelectronic switch functioning as a quantum-interference-effect transistor. *Physical Review Letters, 109*, 186801. https://doi.org/10.1103/physrevlett.109.186801

Jia, D., Manz, J., & Yang, Y. (2019). De- and recoherence of charge migration in ionized iodoacetylene. *The Journal of Physical Chemistry Letters, 10*, 4273–4277. https://doi.org/10.1021/acs.jpclett.9b01687

Kanno, M., Abe, M., Nakajima, T., Hoki, K., & Fujimura, Y. (2006). Control of π-electron rotation in chiral aromatic molecules by nonhelical laser pulses. *Angewandte Chemie International Edition, 45*, 7995–7998. https://doi.org/10.1002/anie.200602479

Krause, P., Klamroth, T., & Saalfrank, P. (2005). Time-dependent configuration-interaction calculations of laser-pulse-driven many-electron dynamics: Controlled dipole switching in lithium cyanide. *The Journal of Chemical Physics, 123*, 074105. https://doi.org/10.1063/1.1999636

Kumar, B. G., & Prakash, K. S. (2021). Nanoelectronics and photonics for next-generation devices. In the *Handbook of polymer and ceramic nanotechnology* (p. 293). Springer.

Mineo, H., Lin, S.-H., & Fujimura, Y. (2013). Coherent π-electron dynamics of (P)-2,2′-biphenol induced by ultrashort linearly polarized UV pulses: Angular momentum and ring current. *The Journal of Chemical Physics, 138*, 074304. https://doi.org/10.1063/1.4790595

Mineo, H., & Fujimura, Y. (2017). Quantum control of coherent π-electron ring currents in polycyclic aromatic hydrocarbons. *The Journal of Chemical Physics, 147*, 224301. https://doi.org/10.1063/1.5004504

Mineo, H., Yamaki, M., Teranishi, Y., & co-authors. (2012). Quantum switching of π-electron rotations in a nonplanar chiral molecule by using linearly polarized UV laser pulses. *Journal of the American Chemical Society, 134*, 14279–14282. https://doi.org/10.1021/ja3047848

Mohammed, H., Mia, M. F., Wiggins, J., & Desai, S. (2025). Nanomaterials for energy storage systems—A review. *Molecules, 30*, 883. https://doi.org/10.3390/molecules30040883

Nobusada, K., & Yabana, K. (2007). Photoinduced electric currents in ring-shaped molecules by circularly polarized laser. *Physical Review A, 75*, 032518. https://doi.org/10.1103/PhysRevA.75.032518

Steiner, E., & Fowler, P. W. (2001). Patterns of ring currents in conjugated molecules: A few-electron model based on orbital contributions. *The Journal of Physical Chemistry A, 105*, 9553–9562. https://doi.org/10.1021/jp011955m

Steiner, E., Soncini, A., & Fowler, P. W. (2005). Ring currents in the porphyrins: π-shielding, delocalisation pathways and the central cation. *Organic & Biomolecular Chemistry, 3*, 4053–4059. https://doi.org/10.1039/b511913h

Ulusoy, I. S., & Nest, M. (2011). Correlated electron dynamics: How aromaticity can be controlled. *Journal of the American Chemical Society, 133*, 20230–20236. https://doi.org/10.1021/ja206193t.

CHUYỂN ĐỘNG QUAY KẾT HỢP CỦA π-ELECTRON TRONG MỘT PHÂN TỬ THƠM NHỎ

Hồ Quang Huy

Khoa Kỹ Thuật Công Nghệ, Trường Đại học Phan Thiết, Lâm Đồng, Việt Nam

Tóm tắt: *Chuyển động quay kết hợp là một kiểu di cư điện tích điển hình trong các phân tử hydrocarbon thơm, trong đó π-electron quay dọc theo mạch vòng phân tử. Trong khuôn khổ của cơ học lượng tử, chuyển động quay của π-electron có thể được đặc trưng bởi giá trị trung bình của một số đại lượng có khả năng quan sát, như một thành phần động lượng góc hoặc mật độ dòng. Những đại lượng này hoàn toàn có thể được đánh giá bằng các biểu thức giải tích kết hợp với phương pháp tính toán hoá lượng tử ab-initio được thực hiện bằng phần mềm Gaussian, trong một công bố của H. Mineo và cộng sự (2013); Đây là một hướng tiếp cận có khả năng mở rộng cho nhiều hệ thơm có kích thước khác nhau. Trong báo cáo này, chúng tôi áp dụng hướng tiếp cận nêu trên để khảo sát chuyển động quay kết hợp của π-electrons trong một phân tử thơm đơn giản, s-triazine ($C_3H_3N_3$), thuộc nhóm điểm đối xứng D_{3h}. Dòng điện vòng không chỉ xuất hiện trên mạch chỉ chứa cặp carbon-carbon, hoặc nitrogen-nitrogen, mà còn trên mạch vòng phân tử chức các cặp carbon-nitrogen nằm liền kề nhau. Độ lớn của mỗi dòng điện trên liên kết được xác định thông qua tổng thông lượng xuyên qua mặt phẳng đặt ở điểm chính giữa của đường nối hai tâm nguyên tử. Để dễ dàng hình dung sự bố trong không gian của mật độ dòng điện, một biểu đồ mật độ dòng được vẽ trên mặt phẳng nằm song song với mặt phẳng chính của phân tử và cách đó z=1.0 Å.*

Từ khóa: *chuyển động quay kết hợp, phân tử thơm, π-electron*

Thông tin tác giả:

ThS. Hồ Quang Huy *(*Tác giả liên hệ)*, Khoa Kỹ thuật Công nghệ, Trường Đại học Phan Thiết, Lâm Đồng, Việt Nam.

Email: hqhuy@upt.edu.vn

Ghi chú

Tác giả xác nhận không có tranh chấp về lợi ích đối với bài báo này.